Uptake and Distribution of Silver in the Aquatic Plant *Landoltia punctata* (Duckweed) Exposed to Silver and Silver Sulfide Nanoparticles

John P. Stegemeier,[1,2]† Benjamin P. Colman,[1,3,4]† Fabienne Schwab,[1,5,6] Mark R. Wiesner,[1,6]

*and Gregory V. Lowry[1,2]**

1 Center for the Environmental Implications of NanoTechnology (CEINT)

2 Civil & Environmental Engineering, Carnegie Mellon University, Pittsburgh, PA 15213, United States

3 Department of Biology, Duke University, Durham, NC 27708, United States

4 Current address: University of Montana, Department of Ecosystem and Conservation Sciences, Missoula, MT

5 Current address: Aix-Marseille Université, CNRS, IRD, CEREGE UM34, 13545 Aix en Provence, France

6 Civil & Environmental Engineering, Duke University, Durham, NC 27708, United States

†equal contribution

*corresponding author: Gregory V. Lowry, glowry@cmu.edu, +1 (412) 268-2948

Keywords: heavy metals, nanoparticles, fate, uptake, pollution, environmental nanotechnology, bioaccumulation, bioavailability, colloidal silver, phytoremediation, macrophytes

Abstract

Aquatic ecosystems are expected to receive Ag^0 and Ag_2S nanoparticles (NPs) through anthropogenic waste streams. The speciation of silver in Ag-NPs affects their fate in ecosystems, but its influence on interactions with aquatic plants is still unclear. Here, the Ag speciation and distribution was measured in an aquatic plant, duckweed (*Landoltia punctata*), exposed to Ag^0 or Ag_2S NPs, or to $AgNO_3$. The silver distribution in duckweed roots was visualized using synchrotron-based micro X-ray fluorescence (XRF) mapping and Ag speciation was determined using extended X-ray absorption fine structure (EXAFS) spectroscopy. Duckweed exposed to Ag_2S-NPs or Ag0-NPs accumulated similar Ag concentrations despite an order of magnitude smaller dissolved Ag fraction measured in the exposure medium for Ag_2S-NPs compared to Ag^0-NPs. By twenty-four hours after exposure, all three forms of silver had accumulated on and partially in the roots regardless of the form of Ag exposed to the plants. Once associated with duckweed tissue, Ag^0-NPs had transformed primarily into silver sulfide and silver thiol species. This suggests that plant defenses were active within or at the root surface. The Ag_2S-NPs remained as Ag_2S, while $AgNO_3$ exposure led to Ag^0 and sulfur-associated Ag species in plant tissue. Thus regardless of initial speciation, Ag was readily available to duckweed.

TOC Art:

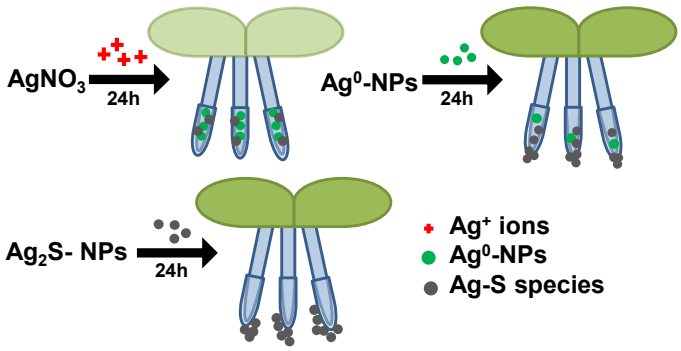

1. Introduction

Engineered nanomaterials (ENMs) are a class of pollutants of emerging concern in aquatic ecosystems released either directly (*e.g.,* wastewater effluent), or indirectly (*e.g.,* through the erosion of land-applied biosolids).[1-3] Silver nanoparticles (Ag^0-NPs) are of particular concern as they are used as an antibiotic in many commercial nano-enabled products and have been well documented as toxic to aquatic[4] and terrestrial organisms.[5, 6] Understanding the environmental fate of these ENMs is needed to better characterize environmental exposures to Ag^0-NPs. Considering pristine ENMs in natural systems is necessary but not sufficient, as they are subject to a complex range of transformations, which can influence their fate, mobility in soils, solubility, and bioavailability, as well as their toxicity.[2, 3, 7-12] While Ag_2S-NPs are much less soluble[6, 13, 14] than metallic silver ENMs, transformations between Ag_2S, Ag^+ and Ag^0, and formation of new Ag^0-NPs can occur under environmentally relevant conditions.[15, 16] In wastewater and land-applied biosolids, most of the Ag^0-NPs and other nanoparticles (*e.g.,* ZnO-NPs), can be transformed into their less reactive metal sulfide equivalents (Ag_2S-NPs, ZnS-NPs, etc.).[17-20] In the case of silver, Ag_2S can account for more than 90% of the Ag in the wastewater treatment plant biosolids.[13, 20] In aquatic environments such as wetlands, the dissolution and precipitation dynamics of Ag^0-NPs is highly complex,[15] and the factors that influence ENM interactions with aquatic plants remain poorly characterized.[21]

Plants play a central role in aquatic ecosystems, providing food, moderating flow regimes, and driving ecosystem biogeochemistry through oxygen production and removing excess nutrients; plants also are strongly involved in metal and ENM cycling.[21-24] In aquatic plants, ENMs are expected to adsorb onto the surface as well as be taken up.[25, 26] Although

smaller particles are generally more rapidly internalized by plants, many other factors may drive plant uptake of ENMs including ENM composition and exposure conditions.[21, 25, 27, 28] While plants are known to take up both dissolved metals and nanoparticles, some evidence suggests dissolved metals may be taken up more readily.[29] This then suggests that the solubility of a metal or metal oxide nanomaterial could greatly affect the dominant uptake pathway as well as the extent and rate of uptake. Thus highly soluble ENMs would be expected to dissolve and yield greater uptake and translocation than less soluble ENMs which might tend to attach to the outsides of the roots, or be taken up as intact nanoparticles as was observed in a terrestrial plant (alfalfa) exposed hydroponically to ionic Ag and to less soluble Ag-NP species.[27]

The goal of the present study was to study the interaction of ENMs with aquatic plants in order to: a) determine the differences in uptake of Ag^{+}, Ag^{0}-NPs and Ag_2S-NPs; and b) qualitatively elucidate and compare the route of uptake and speciation of these three silver forms as they were taken up into plant tissues by using synchrotron based X-ray techniques. We chose the aquatic plant *Landoltia punctata* to use as it is a member of group of small floating aquatic plants ("duckweeds"; also includes the genera *Lemna* and *Spirodela*) which are common model organisms for assessing the toxicity of contaminants,[30] including Ag^{0}-NPs[31]. Their small size, rapid growth rate, and propensity for accumulating large concentrations of metals also make them ideal for studies on the fate and transport of metal and metal oxide ENMs. Moreover, duckweeds are a promising tool for (ENM) phytoremediation.[32, 33]

2. Materials and Methods

2.1 Synthesis

Polyvinylpyrrolidone (PVP) coated Ag^0-NPs were synthesized based on a protocol of Yang and co-workers,[34] and a part of these Ag^0-NPs was oxidized and reacted with inorganic sulfide to form Ag_2S-NPs as described by Reinsch and co-workers,[35] and adapted elsewhere.[27] In brief, 1.5g of PVP (1000 g/mol) was dissolved in 280 mL of deionized water before stirring in 9 mL of 0.10M $AgNO_3$ for five minutes. Under constant stirring, 11 mL of ice-cold 0.08M $NaBH_4$ was added, allowed to react for one hour, and washed as described below, resulting in the final stock suspension of Ag^0-NPs.[27] The Ag_2S-NPs were synthesized from a second batch of Ag^0-NPs by adding 9 mL of 0.10 M Na_2S into an aqueous suspension of Ag^0-NPs bubbled with aquarium air pumps (AP 200, Tetratec, China) to provide dissolved oxygen, and allowed to react for one week before washing. Both NP suspensions were washed three times using ultracentrifugation (50,000×*g* for 30 min) and resuspension in deionized water using a sonicating probe (Sonic Dismembrator Model 550, Fisher Scientific, USA, power level 3, 1 min). Washed suspensions were stored at 4 ºC until use.

2.2 Characterization

Two batches of each type of NP (Ag^0 and Ag_2S) were synthesized as described above (once for each exposure corresponding to the synchrotron schedule). The first batch of washed Ag^0-NPs and Ag_2S-NPs was characterized in detail by Transmission Electron Microscopy (TEM), X-ray diffraction (XRD), and dynamic light scattering (DLS). The second batch was analyzed by DLS to confirm similarity between batches. The crystalline phase was verified by XRD of an air-dried sample using an X-Radia XRD (X'Pert Pro MPD X-ray diffractometer with

a Cu X-ray source). The XRD spectra were background-subtracted and peak-matched using X'pert Highscore Plus software. The morphology and diameter of the unfiltered NPs were determined by TEM imaging of samples dried on Formvar coated copper grids using a TECNAI G^2 Twin (FEI, Hillsboro OR, USA). The hydrodynamic diameter and zeta potential, calculated using the Smoluchowski equation, of a 20µm filtered NP suspension was determined in 10 ppm Ag^0-NP suspension in the duckweed growth medium (half strength Hutner's solution) using an ALV/CGS-3 (ALV, Germany) and a Zetasizer Nano ZS (Malvern, UK), for the first and second batches, respectively. The hydrodynamic diameter was measured at t=0 h and again after 48 h in the growth chamber exposed to cool fluorescent light (see below) to assess the stability of the NPs against aggregation in the growth medium under the conditions of the exposure. Finally, the soluble fraction of silver was determined in the suspensions after 48 h in half strength Hutner's medium using a 3 kDa centrifuge filter to separate the particles from the dissolved species.

2.3 Exposure of Duckweed to Ag^0 and Ag_2S Nanoparticles

Two batches of semi-sterile cultures of duckweed (*L. puctata*) were stabilized in half strength Hutner's medium and exposed to the NPs using a method adapted from Brain and co-workers 2007,[36] one for the XRF mapping and another for the EXAFS analysis. Twenty specimens of *L. punctata*, each containing three developed fronds (a mother and two 1st-generation daughter fronds) were exposed in 25 mL plastic Petri dishes (Supporting Information [SI], Figure S1). To prepare the exposure medium, suspensions of Ag^0-NPs, Ag_2S-NPs or $AgNO_3$ were added to 20 mL of growth medium to achieve 10 ppm total silver concentration. This concentration is much higher than likely environmental exposures, but was necessary to provide sufficient signal for both XRF mapping and EXAFS analysis. Dishes were placed in a

reflective aluminum tray and covered with another aluminum tray which had holes cut for the two cool fluorescent lights placed approximately 15 cm from the duckweed (Figure S1). The cultures were harvested 24 h after exposure, and immediately rinsed by agitating and transferring the cultures in two consecutive Petri dishes containing DI water using a sterile fork. This washing step served to remove any loosely bound particles and any ionic silver associated with the exposure medium. The silver remaining in the duckweed tissue after this washing step is termed sorbed (including ad- and absorption; no differentiation between adhered and internalized Ag was made). Several specimens were collected after 24 and 60 h of exposure, and prepared by sealing fresh plant tissue immersed in water inside plastic sample holders sealed within Kapton tape. Due to the water tight sealing, the samples remained hydrated during the XRF mapping. Additional tissue samples were immediately frozen in liquid nitrogen and lyophilized for X-ray absorption spectroscopy (XAS) analysis to determine Ag speciation, and a portion was digested in concentrated nitric acid for 24 h on an end-over-end rotator and was then used for total Ag analysis by ICP-MS after dilution with DI water to 5% nitric acid and analyzed (n=1) using a 5-point single element (Ag) calibration standard. The exposure medium was also collected and analyzed (n=2) for total silver to determine the fraction of added silver that was associated with the plant tissues and to calculate a mass balance (75-90%) for silver.

2.4 Silver Speciation

The Ag speciation in the freeze-dried duckweed was investigated by pressing the tissue into pellets and subsequent Ag K-edge XAS analysis. Extended X-ray absorption fine structure (EXAFS) spectra were collected on beamline 11-2 at Stanford Synchrotron Radiation Lightsource (SSRL). The Si(111) crystal monochromator was calibrated by setting the first

inflection of the Ag K-edge of the Ag reference foil to 25,514 eV. The monochromator was detuned to 75% of its maximum to reduce harmonics and the spectra for the exposed duckweed samples were collected in fluorescence mode using a 100-element solid state Ge detector. To ensure an optimal energy calibration, the spectrum of the reference Ag foil was simultaneously collected in transmission mode between ion chambers filled with Ar. Each sample was scanned 3-5 times (300-500 individual spectra) to maxize data quality.

All spectra were averaged and analyzed using the Athena software package.[37] Background was corrected and the E_0 set to 25,534 eV. The sample spectra were fitted by linear combination fitting (LCF) of averaged k^3- weighted EXAFS spectra. The EXAFS data was fitted over k = 2-9.5 Å^{-1} using a variety of Ag model compounds.[35] A complete list of the model compounds used is presented in Table S1 (SI). The fits were not constrained to 100% and utilized the cycle-fit method: finding the best 1-component fit, and adding another component if the R-factor is decreased by 10% through addition of that compound. The R-factor is a goodness-of-fit parameter and lower values indicate better fits; although this parameter depends on the fitting range, a 10% decrease is used to indicate a significant improvement to the fit because principal component analysis (PCA) and target transform (TT) were not possible due to the low number of samples.

2.5 Silver Distribution

To spatially resolve the silver in the duckweed plant tissue, synchrotron XRF microprobe mapping was conducted on the IDE-13 beamline at the synchrotron-radiation light source research facility Advanced Photon Source (APS, Argonne IL, United States). An incident beam with an excitation energy of 28,000 eV was used to maximize the silver K-edge fluorescence

signal. This produced a 2.5x2.5 μm beam which was scanned across the root tip with a 2 μm step size and 20 ms dwell time. A 4-element vortex silicon drift detector was placed normal to the incident beam with the sample mounted in the 45-degree geometry. Signals from Ag and Zn were calibrated using standards and integrated from the multiple channel analysis by fitting the K-edge fluorescence peaks. The signals from each element were normalized with I_0 to produce element specific maps. Silver specific maps were obtained using the Ag K-α emission line (22,163 eV) and processed with the X-ray Data Browser software provided by the APS. Zinc specific maps are shown in the Figure S2 in the SI.

3. Results and Discussion

3.1 Characterization

The NP characterization including the hydrodynamic diameters and the zeta potential measured in the half strength Hutner's growth medium, the TEM diameters, and the XRD analysis are provided in Table 1. The crystalline phases identified by XRD were body-centered cubic metallic silver in the Ag^0-NP and acanthite (Ag_2S) in the Ag_2S-NP, suggesting that complete sulfidation had been achieved with the sulfidation method used. The particles were spheroidal, with primary particle sizes determined by TEM of 6.3 and 7.8 nm for the Ag^0-NPs and Ag_2S-NPs, respectively (SI Figure S3). The number-averaged hydrodynamic diameter of the freshly prepared and 0.2μm filtered Ag^0-NP and Ag_2S-NP in half strength Hutner's media determined by DLS was found to be 13.4±2.9 and 17.9±2.4 nm for the respectively. The hydrodynamic diameter determined in half strength Hutner's medium is larger than the TEM diameter, likely due to the presence of an electron transparent PVP coating invisible in TEM but affecting the diffusion coefficient and hence hydrodynamic diameter, and potentially also due to

aggregation. However, the particle size was found to be relatively constant after two days in the growth medium 14.4±4.0 and 20.3±0.6nm for the Ag^0-NPs and Ag_2S-NPs, respectively. An example of the size distribution and autocorrelation function are provided in Figure S4 (SI). Because ion uptake is known to be a major pathway of metal uptake, the solubility of the NPs is expected to influence the uptake of silver. The soluble fraction of silver after two days in half strength Hutner's medium was 0.53 and 0.06 ppm soluble silver for the 10 ppm suspension of Ag^0-NPs and Ag_2S-NPs, respectively. This is consistent with expectations and previous finding showing that Ag_2S is the less soluble form of the silver NPs.[27, 38-40] The three treatments ($AgNO_3$, Ag^0, Ag_2S) spanned four orders of magnitude of soluble silver which will highlight the differences between ion and NP uptake into the plants.

3.2 Silver Concentrations in Tissue

The total silver concentrations sorbed to the bulk lyophilized duckweed tissue exposed to Ag_2S-NPs, Ag^0-NPs, or $AgNO_3$ were measured after 24 h. The total silver includes both silver attached onto the exterior (adsorbed Ag) of the plants and internalized silver (absorbed Ag). The silver concentrations that accumulated in the duckweed exposed to Ag_2S-NPs and Ag^0-NPs were similar, 372±6 and 389±3 ppm Ag respectively (dry weight). The plants exposed to $AgNO_3$ contained nearly twice the silver concentration (685 ±6 ppm Ag) as the NP-exposed samples. Clearly, the Ag ions were more readily (almost two times more) accessible than the particulate forms of Ag. However, the silver concentrations in duckweed exposed to Ag^0- and Ag_2S-NPs did not follow the trends in the measured dissolved silver fractions: they contained similar

concentrations of silver despite the almost 10 times more dissolved silver with the Ag^0-NPs compared to Ag_2S-NPs (Table 1). Two possible processes, which likely occurred in combination, can explain these observations. Similar concentrations would result if particle attachment and/or direct NP uptake were the primary mode of NP interaction with duckweed roots, rather than uptake of Ag^+ ions or other dissolved Ag forms. However, these are dynamic systems affected by all of the NP behaviors (attachment, uptake, and dissolution) and the plant's response. Thus, the combination of oxidative dissolution of Ag^0-NPs and subsequent uptake/toxicity of Ag^+, and NP attachment, could have coincidentally resulted in similar Ag content in the plant roots. These two explanations are explored further using XRF mapping to look at the distribution of Ag in the plant roots as discussed later in the paper.

In all cases, only 1-2 % of the total silver added was sorbed to the plant tissue. The majority of the silver remained in the exposure medium given the low plant mass to medium volume used (20 duckweed plants in 25 mL, similar to a natural population of duckweed in a pond). While other studies have shown that duckweed can remove >60% of total Zn and Cu within two days, the total biomass-to-metal ratio was much higher in those studies,[33] and in outdoor mesocosm experiments containing more environmentally relevant populations of duckweed, the percentage of total Ag accumulating in aquatic plants was much lower (0.2%). The total Ag recovery in the experimental system (including plant tissue, exposure media, and an aqua regia wash of the exposure vessel) was 75-90% (data not shown). A bioconcentration factor (BCF) for the one day exposure to 10 ppm Ag was estimated by dividing the wet weight concentration by the exposure concentration, assuming 95% water weight for duckweed.[41] The

BCF was ~3 for $AgNO_3$, and ~2 for the NPs (based on wet weight), suggesting that duckweed concentrates and accumulates silver in its tissue.

3.3 Silver Distribution

The silver Kα XRF maps of hydrated root tips exposed to $AgNO_3$, Ag^0-NPs and Ag_2S-NPs demonstrate clear differences in the distribution of Ag for each type of Ag used (Figure 1). Note that each image is color-scaled internally using the highest Ag counts in the image. The scale is affected by both total Ag concentration and its distribution so direct comparisons of Ag concentration between images based on intensities cannot be made. The maximum Ag count used to calibrate each image is provided in Table S2 (SI). Note that very little silver was detected in the initial Ag specific maps for the fronds compared to the roots (SI Figure S5). This conflicts with other reports of metal uptake by duckweed where most of the metal uptake was found to occur in the fronds. The difference in Ag uptake behavior may be a result of the different species being investigated: Here we are looking at uptake by *L. punctata*, which is known to uptake metals through the roots.[42, 43] The other studies showing uptake primarily by the fronds used *Spirodela polyrhiza, Lemna gibba* and *Lemna minor.*[44-46] Given the absence of metal in the fronds of *L. punctata*, the mapping focused mainly on the silver-rich root tips.

After 24 h of exposure to $AgNO_3$, the silver was distributed throughout the root tip and showed highest concentrations near the apical meristem (Figure 1). The root cap is visible as a blue shadow around the root tip, indicating that it has adsorbed a relatively small portion of silver. This Ag distribution pattern suggests Ag^+ ions are able to migrate into the active zone of root tip and do not appear to be restricted by the root cap. For both types of investigated Ag-NPs, the attachment onto the root surface was expected to be similar given their similar size, zeta

potential, and PVP coating (Table 1). However, the Ag maps in Figure 1 show that the uptake behavior was different. The root tip exposed to Ag^0-NPs for 24h shows a similar distribution of Ag as the $AgNO_3$-exposed samples, suggesting that at least a portion of the NPs dissolve prior to entering the root tip. Additionally, there are hotspots of Ag located at the tip of the root cap, suggesting attachment of a solid silver phase, likely Ag^0-NPs. The primary route of Ag^0-NP uptake into these plant roots appears to be through attachment onto the root surface (root cap), dissolution assisted by the acidic local environment in root cap mucilage, and internalization (and possibly re-precipitation) of dissolved silver. Direct uptake of pristine or sulfidized Ag-NPs is likely occurring in parallel (see discussion of the EXAFS results below). In contrast to Ag^0-NPs, the root tip exposed to Ag_2S-NPs shows a hotspot of silver located at the end of the root cap suggesting the silver was not readily internalized. The root cap is visible, indicating the presence of a low Ag concentration throughout the cap, but the absence of silver in the apical meristem shows that little dissolved silver internalized after one day. Due to the small fraction of dissolved Ag, and in view of the EXAFS speciation results discussed below, the primary route of uptake of Ag_2S-NPs appears to be attachment onto the root surface, and direct NP migration into the plant tissue.

After 60 h of exposure to $AgNO_3$, the root tip shows many small Ag hotspots throughout the root tip primarily located near the apical meristem (Figure 1). It is important to note that these are different root samples than the 24 h images and not a progression from the previous images. The duckweed exposed to ionic silver for 60 h was visually lighter (turning white) than the plants of the other treatments, suggesting this level of ionic silver exposure was toxic to the duckweed. Since the reduction, precipitation and sequestration of metals in plant roots are

common responses to high doses of dissolved metals, and in agreement with the EXAFS results below, these Ag hotspots are likely biogenic silver NPs being sequestered in the plant tissue.[47, 48] In contrast, the plants exposed to Ag^0-NPs or Ag_2S-NPs showed no signs of toxicity. The root tip exposed to Ag^0-NPs for 60 h appears similar to the 24h exposed with silver primarily located at the apical meristem and the presence of discrete Ag hotspots adhered to the root cap. Again, this is indicative of NP attachment onto the root surface as well as ionic uptake into the active region of the root tip. The silver sorbed to the root tip exposed to Ag_2S-NPs for 60 h was mostly located near the apical meristem and the early vasculature region. The granular silver distribution suggests limited NP dissolution, or Ag^+ uptake and subsequent re-precipitation. This is in agreement with recent findings in different plants showing that an Ag^+ fraction from Ag_2S-NPs is bioavailable.[6, 27] Given the limitations of two-dimensional maps of three-dimensional roots, these maps cannot prove NP internalization, but the distribution patterns in Figure 1 strongly suggest that the metals from the NPs are not merely attached onto the surface, but have also entered the vascular system. Metal uptake XRF maps for plants have previously been modeled and correlated to specific metal distribution in the plant vasculature (e.g. adhered to outside of root vs. internalized into the vasculature). The pattern in our images is consistent with metal uptake into the plant vasculature.[49]

3.4 Silver Speciation

Normalized EXAFS spectra and their corresponding fits of the three treatments ($AgNO_3$, Ag^0-NPs, and Ag2S-NPs) show clear differences in the Ag absorption spectra (Figure 2 and Table 2). While it is common for Ag EXAFS fits to exceed 100%,[50, 51] we did not force the sums to equal 100% as is often done[6, 38, 52] to preserve the integrity of the fits. All sample spectra fit to

combinations slightly above 100% of the model compounds, which may be a result of the background removal and normalization procedures. Here, the phases and relative amplitudes for each fit match well suggesting that the correct Ag species are identified.

The silver associated with the duckweed tissue exposed to ionic silver was found to be primarily (78%) zero-valent. The EXAFS spectrum from this sample is characteristic for metallic silver particles with strong Ag-Ag scattering giving rise to large oscillations at $k > 7$ Å^{-1}. [20, 35] The presence of metallic Ag could be from the plants native ability to reduce Ag ions to metallic Ag[53]. Metallic silver NPs may have also formed under visible light during the incubation period of the duckweed with the $AgNO_3$, as has been previously reported.[15, 16] However, it cannot be ruled out that metallic Ag formed from the photo-reduction of silver ions or amorphous Ag-S phases in the X-ray beam. For photo-reduction, the existence of metallic silver particles may therefore indicate the presence of silver ions or amorphous Ag-S phases. The larger fraction of metallic Ag in the $AgNO_3$ exposed plants compared to the AgNP exposed plants indicates that there was a greater fraction of photo-reducible Ag for $AgNO_3$. The uniformity of the silver distribution in the root tip compared to the Ag^0-NPs exposed tips, and the lack of Ag hotspots at the root tip suggest that the predominant bioavailable form of silver in the solution exposed to the duckweed was dissolved Ag rather than nanoparticulate. The remaining silver in the silver nitrate exposed roots was sulfur-associated with silver sulfide yielding the best fit. However, it is also likely that thiolated Ag species were present given a known defense mechanisms of plants against oxidative stress via metal toxicity involves thiol production, such as glutathione.[25, 55] The Ag-thiol signal may have also been present but was less than 10% of the total silver or was masked by the presence of the large oscillations of the Ag^0 signal (SI, Figure S6).

In contrast to $AgNO_3$, the majority of the silver from the Ag^0-NP treatment was consistent with sulfur bound Ag, namely a mixture of Ag_2S (64%) and Ag-thiol (53%). Metallic Ag was also present (16%), due either to direct attachment/uptake of NPs onto/into the duckweed, to oxidation of Ag^0 coupled with uptake and in-vivo reduction of dissolved silver, or photo-reduction of available photo-reducible Ag. The differences in speciation between the $AgNO_3$ and Ag^0-NP treatments suggest that the form of Ag entering the plant is different, or that the duckweed may respond differently to the presence of dissolved Ag than to Ag^0-NPs. We hypothesize that in the $AgNO_3$ exposure, acute toxicity (noted from the whitening of the fronds) may have overwhelmed the plant's ability to combat the presence of Ag, while in the Ag^0-NP exposure, the plants can respond with glutathione and other sulfide-based defenses against Ag^+ toxicity.

Based on the bulk EXAFS, silver from the Ag_2S-NP treatment remained as silver sulfide, which suggests that the plant was not able to dissolve or transform a significant amount of the Ag_2S-NPs after 24 h. This is expected for the majority of Ag_2S, given its high chemical stability and low fraction of dissolved silver (Table 1).

4. Implications

The findings of this study have a number of important implications regarding the interactions between metallic NPs and the aquatic plants that are essential to ecosystem function. For hydroponic exposures used here, which is a relevant exposure scenario for floating and submerged aquatic plants, metallic NPs interact with aquatic plants differently than ions of the same metal. As expected, ions are more readily internalized than NPs. Moreover, the distribution

of Ag in duckweed exposed to ion and to NPs was different, and related to the properties of the nanoparticles (i.e. dissolution rate). This in turn led to differences in metal speciation in the roots after 24 h of exposure. Exposure to ionic Ag led to more reducible Ag species within the plant roots (either reduced by the plant of by the X-ray beam), whereas exposure to nanoparticulate Ag led to a higher prevalence of sulfur associated Ag species. These differences in Ag speciation may subsequently affect the health of the plants, and their ability to respond to other chemical insults. Future work should assess differences in toxicity afforded by these forms of Ag.

This study also indicates that nanoparticulate phases of metals readily attach to, and are available to aquatic plants. Silver, even in the poorly soluble Ag_2S species, readily attached to the duckweed roots. Silver attachment was more influenced by the particle properties (size, charge, and coating were the same for both the Ag^0-NPs and the Ag_2S-NPs) than by the solubility. Adhered particles are then taken up to some degree into the plant root vasculature, either after being solubilized or as particles. Although comparable amounts of silver were associated with roots for both the Ag^0-NPs and the Ag_2S-NPs, the amount and rate of uptake will depend on the speciation. In view of the low solubility of Ag_2S-NPs, this finding suggests that particle uptake is occurring to some extent, and is consistent with other reports of uptake of NPs by duckweed species.[45, 56, 57] Overall, this confirms that NPs can be internalized into the plant tissue even if they are not releasing a large fraction of ions.

The use of duckweed for phytoremediation of metals has been proposed.[33] The present results are indeed promising and show that even at high metal concentrations, duckweed can rapidly accumulate concentrations of Ag NPs at least two-fold higher than environmental concentrations in both ionic and particulate form. To further evaluate the phytoremediation

potential of duckweed to remove metal and metal oxide NPs, follow-up studies should focus on quantification of the attachment strength and attachment and internalization rates of NPs to duckweed using higher spatial resolution (nano-scale) techniques.

5. Acknowledgements

We would like to thank Tyler Bray, Tara Soni, Michelle Laura Zeliph, and Elizabeth Yin for their work in setting the groundwork for these studies, and maintaining the cultures of *Landolita punctata*. The material is based upon work supported by the US National Science Foundation (NSF) and the Environmental Protection Agency (EPA) under NSF Cooperative Agreement EF 1266252, Center for the Environmental Implications of NanoTechnology (CEINT), and from the NSF Nanotechnology Environmental Effects and Policy Integrated Graduate Education and Research Traineeship (DGE-0966227). Any opinions, findings, conclusions or recommendations expressed in this material are those of the author(s) and do not necessarily reflect the views of the NSF, or the EPA. This work has not been subjected to EPA review and no official endorsement should be inferred. Portions of this research were carried out at the SSRL beamline 11-2, and APS's IDE-13. Both are national user facilities of the Department of Energy, Office of Basic Energy Sciences. F. Schwab was supported by the Swiss NSF (PBEZP3-140058).

Supporting information available

In the SI, more details on the experimental setup (Figure S1), the Zn distribution in the roots (Figure S2), the NP TEM images (Figure S3), and the NP's DLS (Figure S4), and additional maps and EXAFS data (Figure S5-6, Table S1-2) are given. This information is available free of charge *via* the Internet at http://pubs.acs.org/doi/abs/10.1021/acs.est.6b06491.

References

1. Gottschalk, F.; Sonderer, T.; Scholz, R. W.; Nowack, B., Modeled environmental concentrations of engineered nanomaterials (TiO_2, ZnO, Ag, CNT, fullerenes) for different regions. *Environ. Sci. Technol.* **2009,** *43*, (24), 9216-9222; 10.1021/es9015553
2. Lowry, G. V.; Espinasse, B. P.; Badireddy, A. R.; Richardson, C. J.; Reinsch, B. C.; Bryant, L. D.; Bone, A. J.; Deonarine, A.; Chae, S.; Therezien, M.; Colman, B. P.; Hsu-Kim, H.; Bernhardt, E. S.; Matson, C. W.; Wiesner, M. R., Long-Term Transformation and Fate of Manufactured Ag Nanoparticles in a Simulated Large Scale Freshwater Emergent Wetland. *Environ. Sci. Technol.* **2012,** *46*, (13), 7027-7036; 10.1021/es204608d
3. Pradas del Real, A. E.; Castillo-Michel, H.; Kaegi, R.; Sinnet, B.; Magnin, V.; Findling, N.; Villanova, J.; Carrière, M.; Santaella, C.; Fernández-Martínez, A.; Levard, C.; Sarret, G., Fate of Ag-NPs in Sewage Sludge after Application on Agricultural Soils. *Environ. Sci. Technol.* **2016,** *50*, (4), 1759-1768; 10.1021/acs.est.5b04550
4. Navarro, E.; Piccapietra, F.; Wagner, B.; Marconi, F.; Kaegi, R.; Odzak, N.; Sigg, L.; Behra, R., Toxicity of silver nanoparticles to *Chlamydomonas reinhardtii*. *Environ. Sci. Technol.* **2008,** *42*, (23), 8959-8964; 10.1021/es801785m
5. Ratte, H. T., Bioaccumulation and toxicity of silver compounds: A review. *Environ. Tox. Chem.* **1999,** *18*, (1), 89-108; 10.1002/etc.5620180112
6. Wang, P.; Menzies, N. W.; Lombi, E.; Sekine, R.; Blamey, F. P.; Hernandez-Soriano, M. C.; Cheng, M.; Kappen, P.; Peijnenburg, W. J.; Tang, C.; Kopittke, P. M., Silver sulfide nanoparticles (AgS-NPs) are taken up by plants and are phytotoxic. *Nanotoxicology* **2015**, 9, (8), 1041-1049
7. Reidy, B.; Haase, A.; Luch, A.; Dawson, A. K.; Lynch, I., Mechanisms of Silver Nanoparticle Release, Transformation and Toxicity: A Critical Review of Current Knowledge and Recommendations for Future Studies and Applications. *Materials* **2013,** *6, (6), 2295-2350* 10.3390/ma6062295
8. Starnes, D. L.; Unrine, J. M.; Starnes, C. P.; Collin, B. E.; Oostveen, E. K.; Ma, R.; Lowry, G. V.; Bertsch, P. M.; Tsyusko, O. V., Impact of sulfidation on the bioavailability and toxicity of silver nanoparticles to *Caenorhabditis elegans*. *Environ. Pollut.* **2015,** *196*, 239-246; http://dx.doi.org/10.1016/j.envpol.2014.10.009
9. Levard, C.; Hotze, E. M.; Colman, B. P.; Dale, A. L.; Truong, L.; Yang, X. Y.; Bone, A. J.; Brown, G. E.; Tanguay, R. L.; Di Giulio, R. T.; Bernhardt, E. S.; Meyer, J. N.; Wiesner, M. R.; Lowry, G. V., Sulfidation of Silver Nanoparticles: Natural Antidote to Their Toxicity. *Environ. Sci. Technol.* **2013,** *47*, (23), 13440-13448; 10.1021/es403527n
10. Cornelis, G.; Hund-Rinke, K.; Kuhlbusch, T.; Van den Brink, N.; Nickel, C., Fate and Bioavailability of Engineered Nanoparticles in Soils: A Review. *Crit Rev Env Sci Tec* **2014,** *44*, (24), 2720-2764; Doi 10.1080/10643389.2013.829767
11. Yu, S.-j.; Yin, Y.-g.; Liu, J.-f., Silver nanoparticles in the environment. *Environ. Sci. Proc. Imp.* **2013,** *15*, (1), 78-92; 10.1039/c2em30595j
12. Levard, C.; Hotze, E. M.; Lowry, G. V.; Brown, G. E., Environmental Transformations of Silver Nanoparticles: Impact on Stability and Toxicity. *Environ. Sci. Technol.***2012,** *46*, (13), 6900-6914; 10.1021/es2037405
13. Nowack, B., Nanosilver Revisited Downstream. *Science* **2010,** *330*, (6007), 1054-1055;
14. Devi, G. P.; Ahmed, K. B. A.; Varsha, M. K. N. S.; Shrijha, B. S.; Lal, K. K. S.; Anbazhagan, V.; Thiagarajan, R., Sulfidation of silver nanoparticle reduces its toxicity in

zebrafish. *Aquatic Toxicol.* **2015,** *158*, 149-156; http://dx.doi.org/10.1016/j.aquatox.2014.11.007

15. Badireddy, A. R.; Farner Budarz, J.; Marinakos, S. M.; Chellam, S.; Wiesner, M. R., Formation of Silver Nanoparticles in Visible Light-Illuminated Waters: Mechanism and Possible Impacts on the Persistence of AgNPs and Bacterial Lysis. *Environ. Eng. Sci.* **2014,** *31*, (7), 338-349; 10.1089/ees.2013.0366
16. Yu, S.; Yin, Y.; Zhou, X.; Dong, L.; Liu, J., Transformation kinetics of silver nanoparticles and silver ions in aquatic environments revealed by double stable isotope labeling. *Environ. Sci.: Nano* **2016,** *3*, (4), 883-893; 10.1039/c6en00104a
17. Kim, B.; Park, C.-S.; Murayama, M.; Hochella, M. F., Discovery and characterization of silver sulfide nanoparticles in final sewage sludge products. *Environ. Sci. Technol.* **2010,** *44*, (19), 7509-7514; 10.1021/es101565j
18. Brunetti, G.; Donner, E.; Laera, G.; Sekine, R.; Scheckel, K. G.; Khaksar, M.; Vasilev, K.; De Mastro, G.; Lombi, E., Fate of zinc and silver engineered nanoparticles in sewerage networks. *Water Res.* **2015,** *77*, 72-84; 10.1016/j.watres.2015.03.003
19. Kaegi, R.; Voegelin, A.; Sinnet, B.; Zuleeg, S.; Hagendorfer, H.; Burkhardt, M.; Siegrist, H., Behavior of metallic silver nanoparticles in a pilot wastewater treatment plant. *Environ. Sci. Technol.* **2011,** *45*, (9), 3902-3908; 10.1021/es1041892
20. Ma, R.; Levard, C.; Judy, J. D.; Unrine, J. M.; Durenkamp, M.; Martin, B.; Jefferson, B.; Lowry, G. V., Fate of Zinc Oxide and Silver Nanoparticles in a Pilot Wastewater Treatment Plant and in Processed Biosolids. *Environ. Sci. Technol.***2013,** *48*, (1), 104-112; 10.1021/es403646x
21. Thwala, M.; Klaine, S. J.; Musee, N., Interactions of metal-based engineered nanoparticles with aquatic higher plants: A review of the state of current knowledge. *Environ. Tox. Chem.* **2016**, 35, (7), 1677-1694 10.1002/etc.3364
22. McNear Jr., D. H., The rhizosphere—roots, soil and everything in between. *Nat. Educat. Knowledge* **2013,** *4*, (3), 1;
23. Vymazal, J., *Algae and Element Cycling in Wetlands*. Lewis Publishers: Boca Raton, USA, 1995.
24. Janauer, G. A.; Schmidt-Mumm, U.; Schmidt, B., Aquatic macrophytes and water current velocity in the Danube River. *Ecolog. Eng.* **2010,** *36*, (9), 1138-1145; http://dx.doi.org/10.1016/j.ecoleng.2010.05.002
25. Schwab, F.; Zhai, G.; Kern, M.; Turner, A.; Schnoor, J. L.; Wiesner, M. R., Barriers, Pathways and Processes for Uptake, Translocation, and Accumulation of Nanomaterials in Plants—Critical Review. *Nanotoxicology* **2016,** *10*, (3), 257-278; 10.3109/17435390.2015.1048326
26. Glenn, J. B.; White, S. A.; Klaine, S. J., Interactions of gold nanoparticles with freshwater aquatic macrophytes are size and species dependent. *Environ. Tox. Chem.* **2012,** *31*, (1), 194-201; 10.1002/etc.728
27. Stegemeier, J. P.; Schwab, F.; Colman, B. P.; Webb, S. M.; Newville, M.; Lanzirotti, A.; Winkler, C.; Wiesner, M. R.; Lowry, G. V., Speciation Matters: Bioavailability of Silver and Silver Sulfide Nanoparticles to Alfalfa (*Medicago sativa*). *Environ. Sci. Technol.* **2015,** *49*, (14), 8451-8460; 10.1021/acs.est.5b01147
28. Judy, J. D.; McNear, D. H.; Chen, C.; Lewis, R. W.; Tsyusko, O. V.; Bertsch, P. M.; Rao, W.; Stegemeier, J.; Lowry, G. V.; McGrath, S. P.; Durenkamp, M.; Unrine, J. M., Nanomaterials in Biosolids Inhibit Nodulation, Shift Microbial Community Composition,

and Result in Increased Metal Uptake Relative to Bulk/Dissolved Metals. *Environ. Sci. Technol.* **2015,** *49*, (14), 8751-8758; 10.1021/acs.est.5b01208
29. Ebbs, S. D.; Bradfield, S. J.; Kumar, P.; White, J. C.; Musante, C.; Ma, X., Accumulation of zinc, copper, or cerium in carrot (*Daucus carota*) exposed to metal oxide nanoparticles and metal ions. *Environ. Sci. Nano 2016, 3, (1), 114-126* 10.1039/c5en00161g
30. OECD, *Test No. 221: Lemna sp. Growth Inhibition Test*. OECD Publishing.
31. Kim, E.; Kim, S.-H.; Kim, H.-C.; Lee, S.; Lee, S.; Jeong, S., Growth inhibition of aquatic plant caused by silver and titanium oxide nanoparticles. *Toxicol. Environ. Health Sci.* **2011,** *3*, (1), 1-6; 10.1007/s13530-011-0071-8
32. Colman, B. P.; Espinasse, B.; Richardson, C. J.; Matson, C. W.; Lowry, G. V.; Hunt, D. E.; Wiesner, M. R.; Bernhardt, E. S., Emerging Contaminant or an Old Toxin in Disguise? Silver Nanoparticle Impacts on Ecosystems. *Environ. Sci. Technol.* **2014,** *48*, (9), 5229-5236; 10.1021/es405454v
33. Landesman, L.; Fedler, C.; Duan, R., Plant Nutrient Phytoremediation Using Duckweed. In *Eutrophication: causes, consequences and control*, Ansari, A. A.; Singh Gill, S.; Lanza, R. G.; Rast, W., Eds. Springer Netherlands: Dordrecht, 2011; pp 341-354.
34. Yang, X.; Gondikas, A. P.; Marinakos, S. M.; Auffan, M.; Liu, J.; Hsu-Kim, H.; Meyer, J. N., Mechanism of Silver Nanoparticle Toxicity Is Dependent on Dissolved Silver and Surface Coating in *Caenorhabditis elegans*. *Environ. Sci. Technol.* **2012,** *46*, (2), 1119-1127; 10.1021/es202417t
35. Reinsch, B. C.; Levard, C.; Li, Z.; Ma, R.; Wise, A.; Gregory, K. B.; Brown, G. E.; Lowry, G. V., Sulfidation of Silver Nanoparticles Decreases *Escherichia coli* Growth Inhibition. *Environ. Sci. Technol.* **2012,** *46*, (13), 6992-7000; 10.1021/es203732x
36. Brain, R. A.; Solomon, K. R., A protocol for conducting 7-day daily renewal tests with *Lemna gibba*. *Nat. Protocols* **2007,** *2*, (4), 979-987;
37. Ravel, B.; Newville, M., ATHENA, ARTEMIS, HEPHAESTUS: data analysis for X-ray absorption spectroscopy using IFEFFIT. *J. Sync. Rad.* **2005,** *12*, (4), 537-541; doi:10.1107/S0909049505012719
38. Levard, C.; Reinsch, B. C.; Michel, F. M.; Oumahi, C.; Lowry, G. V.; Brown, G. E., Sulfidation processes of PVP-coated silver nanoparticles in aqueous solution: impact on dissolution rate. *Environ. Sci. Technol.* **2011,** *45*, (12), 5260-5266; 10.1021/es2007758
39. Judy, J. D.; Kirby, J. K.; Creamer, C.; McLaughlin, M. J.; Fiebiger, C.; Wright, C.; Cavagnaro, T. R.; Bertsch, P. M., Effects of silver sulfide nanomaterials on mycorrhizal colonization of tomato plants and soil microbial communities in biosolid-amended soil. *Environ. Pollut.* **2015,** *206*, 256-263; http://dx.doi.org/10.1016/j.envpol.2015.07.002
40. Sekine, R.; Brunetti, G.; Donner, E.; Khaksar, M.; Vasilev, K.; Jämting, Å.; Scheckel, K. G.; Kappen, P.; Zhang, H.; Lombi, E., Speciation and lability of Ag-, AgCl- and Ag2S-nanoparticles in soil determined by X-ray absorption spectroscopy and Diffusive Gradients in Thin Films. *Environ. Sci. Technol.* **2015,** 49, (2), 897-905.10.1021/es504229h
41. Bonomo, L.; Pastorelli, G.; Zambon, N., Advantages and limitations of duckweed-based wastewater treatment systems. *Wat. Sci. Technol.* **1997,** *35*, (5), 239-246; http://dx.doi.org/10.1016/S0273-1223(97)00074-7
42. Lalau, C.; Mohedano, R.; Schmidt, É.; Bouzon, Z.; Ouriques, L.; dos Santos, R.; da Costa, C.; Vicentini, D.; Matias, W., Toxicological effects of copper oxide nanoparticles on the growth rate, photosynthetic pigment content, and cell morphology of the duckweed *Landoltia punctata*. *Protoplasma* **2015,** *252*, (1), 221-229; 10.1007/s00709-014-0671-7

43. Lahive, E.; O'Halloran, J.; Jansen, M. A. K., Frond development gradients are a determinant of the impact of zinc on photosynthesis in three species of *Lemnaceae*. *Aquat. Bot.* **2012,** *101*, (0), 55-63; http://dx.doi.org/10.1016/j.aquabot.2012.04.003
44. Upadhyay, R.; Panda, S. K., Zinc reduces copper toxicity induced oxidative stress by promoting antioxidant defense in freshly grown aquatic duckweed *Spirodela polyrhiza* L. *J. Haz. Mat.* **2010,** *175*, (1–3), 1081-1084; http://dx.doi.org/10.1016/j.jhazmat.2009.10.016
45. Farrag, H. F., Evaluation of the Growth Responses of *Lemna gibba* L. (duckweed) Exposed to Silver and Zinc Oxide Nanoparticles. *World App. Sci. J.* **2015,** *33*, (2), 190-202; 10.5829/idosi.wasj.2015.33.02.83
46. Uysal, Y., Removal of chromium ions from wastewater by duckweed, *Lemna minor* L. by using a pilot system with continuous flow. *J. Haz. Mat.* **2013,** *263, Part 2*, 486-492; http://dx.doi.org/10.1016/j.jhazmat.2013.10.006
47. Marchiol, L.; Mattiello, A.; Poscic, F.; Giordano, C.; Musetti, R., In vivo synthesis of nanomaterials in plants: location of silver nanoparticles and plant metabolism. *Nanoscale Res. Let.* **2014,** *9*, (1), 101;
48. Prasad, B. S. N.; Padmesh, T., Common duckweed (*Lemna minor*) assisted green synthesis of silver nanoparticles as potent anti-fungal nanomaterial. *Res. J. Pharm. Technol.* **2015,** *7*, (9), 955-958;
49. Wang, P.; Menzies, N. W.; Lombi, E.; McKenna, B. A.; de Jonge, M. D.; Donner, E.; Blamey, F. P. C.; Ryan, C. G.; Paterson, D. J.; Howard, D. L.; James, S. A.; Kopittke, P. M., Quantitative determination of metal and metalloid spatial distribution in hydrated and fresh roots of cowpea using synchrotron-based X-ray fluorescence microscopy. *Sci. Tot. Environ.* **2013,** *463–464*, (0), 131-139; http://dx.doi.org/10.1016/j.scitotenv.2013.05.091
50. Voegelin, A.; Weber, F.-A.; Kretzschmar, R., Distribution and speciation of arsenic around roots in a contaminated riparian floodplain soil: Micro-XRF element mapping and EXAFS spectroscopy. *Geochim. Cosmochim.Acta* **2007,** *71*, (23), 5804-5820; http://dx.doi.org/10.1016/j.gca.2007.05.030
51. Fulda, B.; Voegelin, A.; Ehlert, K.; Kretzschmar, R., Redox transformation, solid phase speciation and solution dynamics of copper during soil reduction and reoxidation as affected by sulfate availability. *Geochim. Cosmochim.Acta* **2013,** *123*, 385-402; http://dx.doi.org/10.1016/j.gca.2013.07.017
52. Veronesi, G.; Aude-Garcia, C.; Kieffer, I.; Gallon, T.; Delangle, P.; Herlin-Boime, N.; Rabilloud, T.; Carriere, M., Exposure-dependent Ag+ release from silver nanoparticles and its complexation in AgS2 sites in primary murine macrophages. *Nanoscale* **2015,** *7*, (16), 7323-7330; 10.1039/c5nr00353a
53. Gardea-Torresdey, J. L.; Gomez, E.; Peralta-Videa, J. R.; Parsons, J. G.; Troiani, H.; Jose-Yacaman, M., Alfalfa sprouts: A natural source for the synthesis of silver nanoparticles. *Langmuir* **2003,** *19*, (4), 1357-1361; 10.1021/la020835i
54. Thalmann, B.; Voegelin, A.; Sinnet, B.; Morgenroth, E.; Kaegi, R., Sulfidation Kinetics of Silver Nanoparticles Reacted with Metal Sulfides. *Environ. Sci. Technol.* **2014,** *48*, (9), 4885-4892; 10.1021/es5003378
55. Remans, T.; Opdenakker, K.; Guisez, Y.; Carleer, R.; Schat, H.; Vangronsveld, J.; Cuypers, A., Exposure of *Arabidopsis thaliana* to excess Zn reveals a Zn-specific oxidative stress signature. *Environ.Exp. Bot.* **2012,** *84*, (0), 61-71; 10.1016/j.envexpbot.2012.05.005

56. Oukarroum, A.; Barhoumi, L.; Pirastru, L.; Dewez, D., Silver nanoparticle toxicity effect on growth and cellular viability of the aquatic plant *Lemna gibba*. *Environ. Tox. Chem.* **2013,** *32*, (4), 902-907; 10.1002/etc.2131
57. Shi, J.; Abid, A. D.; Kennedy, I. M.; Hristova, K. R.; Silk, W. K., To duckweeds (*Landoltia punctata*), nanoparticulate copper oxide is more inhibitory than the soluble copper in the bulk solution. *Environ. Pollut.* **2011,** *159*, (5), 1277-1282; http://dx.doi.org/10.1016/j.envpol.2011.01.028

Figure Captions

Figure 1. Silver Kα XRF maps of fresh duckweed root tips exposed to $AgNO_3$, Ag^0-NPs and Ag_2S-NPs for 24 and 60 h.

Figure 2. Experiential (black) and linear combination fitted (red) Ag K-edge EXAFS spectra from lyophilized duckweed tissue exposed to $AgNO_3$ (top), Ag^0-NPs (middle) or Ag_2S-NPs (bottom). For clarity, the spectra were plotted with an offset of 5 arbitrary units.

Figures

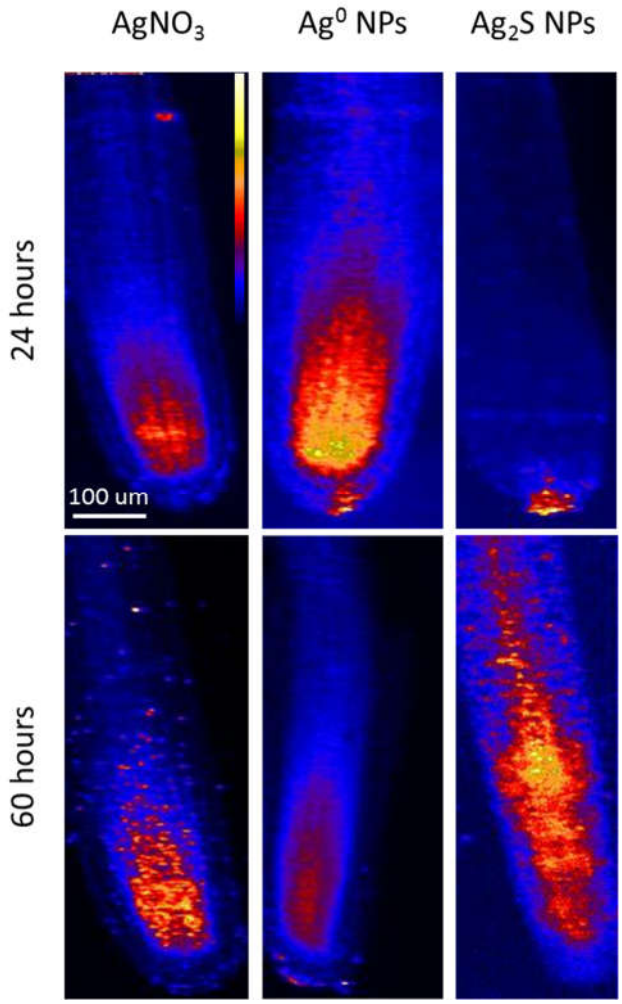

Figure 1. Silver Kα XRF maps of fresh duckweed root tips exposed to $AgNO_3$, Ag^0-NPs and Ag_2S-NPs for 24 and 60 h.

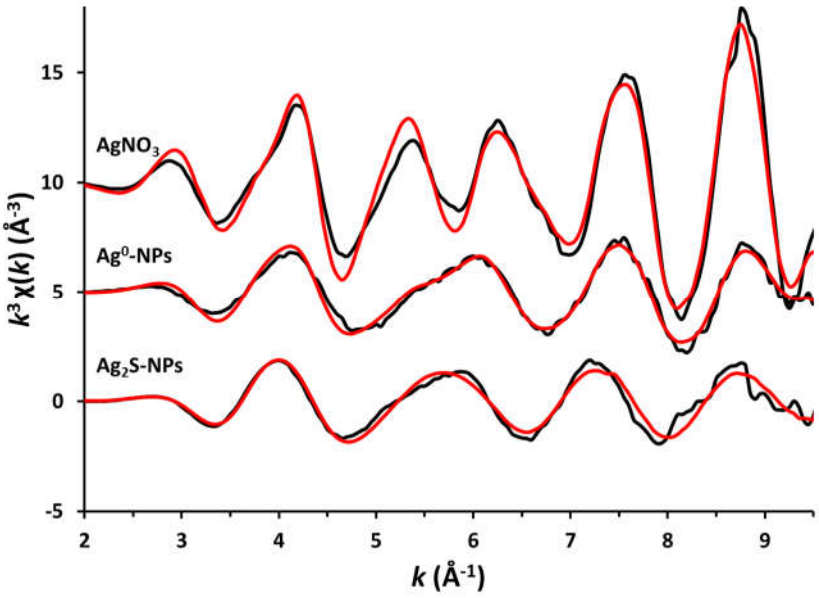

Figure 2. Experiential (black) and linear combination fitted (red) averaged Ag K-edge EXAFS spectra (n=3-5) from lyophilized duckweed tissue exposed to $AgNO_3$ (top), Ag^0-NPs (middle) or Ag_2S-NPs (bottom). For clarity, the spectra were plotted with an offset of 5 arbitrary units.

Table

Table 1. Characterization of freshly prepared Ag^0 and Ag_2S nanoparticles by transmission electron microscopy (TEM) and X-ray diffraction (XRD), and particle properties after suspension in half strength Hutner's medium (hydrodynamic diameter, zeta potential, dissolved Ag). The soluble silver was the fraction of silver in medium without plants than passed a 3 kDa filter after two days.

	Hydrodynamic Diameter (nm)[c]		**Zeta Potential (mV)**	**Dissolved Ag (ppm)**	**TEM size (nm)[a,b]**	**XRD Phase[a]**
Medium	½ Hutner's	½ Hutner's	½ Hutner's	½ Hutner's		
Exp. Time	0 d	2 d	0 d	2 d	-	-
Ag^0-NP	13.4±2.9	14.0±4.0	-11.5±4.8	0.53	6.3±6.2	Silver Metal
Ag_2S-NP	17.9±2.4	20.3±0.6	-10.2±3.8	0.06	7.8±2.2	Acanthite

[a]Data were reproduced from Stegemeier and co-workers 2015[27] where the same NPs were used. [b]Mean plus/minus standard deviation. [c]Number-weighted (primary peak >99% of total number) averaged particle size distribution ± peak width from samples filtered with 0.2 µm cellulose filter.

Table 2. EXAFS linear combination fitting results (fit over *k* of 2-9.5 $Å^{-1}$).

	EXAFS Fitting Results				
Treatment	**Ag^0**	**Ag_2S**	**Ag-Thiol**	**Sum**	**R factor**
$AgNO_3$	78%	39%		116%	0.035
Ag^0-NP	16%	64%	53%	132%	0.032
Ag_2S-NP		127%		127%	0.069